ELSEVIER

FN3: a new protein scaffold reaches the clinic

Laird Bloom and Valerie Calabro

Department of Biological Technologies, Wyeth Research, 87 CambridgePark Drive, Cambridge, MA 02140, USA

In the ten years since the first fibronectin type III (FN3) domain library was published, FN3 has continued to show promise as a scaffold for the generation of stable protein domains that bind to targets with high affinity. A variety of display systems, library designs and affinity maturation strategies have been used to generate FN3 domains with nanomolar to picomolar affinities. The first crystal structures of engineered FN3 molecules in complex with their targets have been solved, and structural studies of engineered FN3 have begun to reveal determinants of stability and to define zones that accept mutations with minimal trade-off between affinity and stability. CT-322, the first engineered FN3 to enter clinical development, is now entering Phase II trials for glioblastoma multiforme.

In 1998, Koide *et al.* published the first account of using an FN3 domain as a scaffold for protein engineering, describing the isolation via phage display of low-affinity ubiquitin binders from a library of molecules with randomized loops [1]. Ten years later, the first patients are being enrolled in a phase II clinical trial of an engineered FN3. Along the way, molecular biology, protein engineering and biophysical studies have begun to demonstrate the flexibility and robust nature of FN3 as a scaffold for the display of binding elements [2–4].

FN3 domains are estimated to be in about 2% of all human proteins and are found in organisms as evolutionarily distant as bacteriophage [5]. The tenth FN3 domain in human fibronectin (^{10}FN3) was first proposed as a scaffold [1] because it combines several features favorable in a molecule intended for therapeutic use. First, FN3 domains are immunoglobulin (Ig)-like domains and adopt a β-fold with noncontiguous loops at the two poles that allow a large binding interface, comparable to those of other scaffolds [6] (Fig. 1a). Further, the hydrophobic core of the Ig fold provides a stable framework structure, imparting an unusually high thermostability to ^{10}FN3 (T_m ~88°C [7,8]). Importantly, and in contrast to variable domains of Igs, ^{10}FN3 is stable as a monomer and lacks cysteine residues and post-translational modifications, which facilitates high-level expression in bacteria. Finally, human plasma fibronectin is normally present at high levels (~300 μg/ml), suggesting minimal potential for immunogenicity from a scaffold based on ^{10}FN3.

Nature has already exploited the functional plasticity of the FN3 fold. A comparison of the crystal structures of more than 50 natural FN3 domains shows a high degree of structural similarity in the seven β-strands (named A–G), while the six loops at the poles (designated AB, BC and so on, based on the β-strands they join) are found in a variety of conformations (Fig. 1a). Binding can occur via loops at either pole (Fig. 1b [9,10]) in contrast to immunoglobulins and T cell receptors, in which binding activity is focused on the pole with the complementarity determining region (CDR) loops (Fig. 1a), while the opposite pole interacts with constant domains. In receptors with FN3-like domains arranged in tandem, loops from adjacent FN3 domains create an extended binding surface (Fig. 1b [9,10]). The binding interfaces between single engineered ^{10}FN3 domains and their protein ligands (699, 733 and 1029 Å^2 [11]; see: 2OCF) are similar in size to those of IgG (mean ~720 Å^2, range 396–1873 Å^2, $n = 45$, see: http://datam.i2r.a-star.edu.sg/BEID) and of single Ig domains, such as the camelid variable domain from single-V_H antibodies (VHH) (mean ~650 Å^2, range 577–793 Å^2, $n = 11$ [12]) and shark immunoglobulin-like novel antigen receptor (IgNAR) (mean ~ 850 Å^2; range 603–1237 Å^2, $n = 5$ [13,14], Fig. 1).

Corresponding author: Bloom, L. (lbloom@wyeth.com)

1359-6446/06/$ - see front matter doi:10.1016/j.drudis.2009.06.007

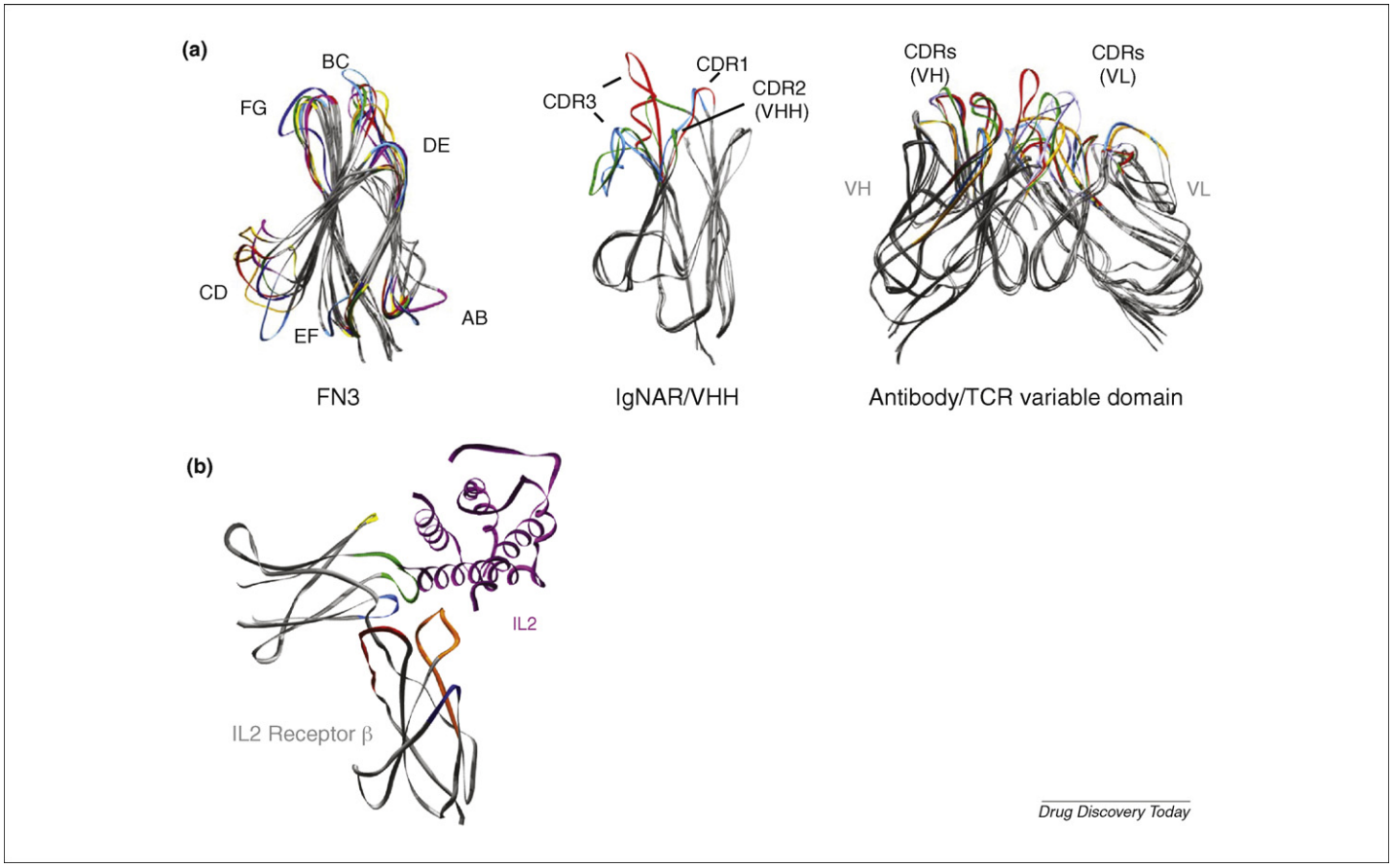

FIGURE 1

Natural Ig fold domain structures. **(a)** Comparison of different Ig fold domains: human FN3 domains, shark IgNAR and camelid VHH domains and variable domains of human antibodies and T cell receptors. Beta strands in the framework of each domain (shown in gray) are aligned with Swiss PDB viewer using the 'iterative fit' option. All loops from a particular molecule are shown in the same color. FN3 domains: second FN3 domain from human ephrin type-B receptor 4 (red; PDB ID 2E7H); ^{10}FN3 (dark blue; PDB ID 1FNA); fourth FN3 domain of human netrin receptor DCC (yellow; PDB ID 2EDB); second FN3 domain of human neogenin (green; PDB ID 1X5G); FN3 domain of human Midline 2 protein (orange; PDB ID 2DMK); sixth FN3 domain of human netrin receptor DCC (purple; PDB ID 2EDE); FN3 domain of human proto-oncogene tyrosine-protein kinase MER precursor (light blue; PDB ID 2DBJ). IgNAR: 5A7 (blue; PDB ID 1SQ2); PBLA8 (red; PDB 1I25). VHH: LLAMA VHH (green; PDB ID 2BSE). Antibodies: Fv domain of a human IgM cryoglobulin (red; PDB ID 1DQL); CBR96 FAB (purple; PDB ID 1CLY), trastuzumab Fab (green; PDB ID 1N8Z) T cell receptor: TCR 5E (blue; PDB ID 2CDF), ELS4 TCR (orange; PDB ID 2NW2). **(b)** IL-2 receptor beta chain in complex with cytokine IL2 (2B5I.pdb). IL-2 receptor α and γ chains have been deleted for clarity. Loops equivalent to those in ^{10}FN3 are color-coded: AB (light blue), BC (orange), CD (yellow), DE (dark blue), EF (green) and FG (red).

Intrinsic properties of FN3

The well-packed hydrophobic core of ^{10}FN3 provides a stable framework structure in the absence of disulfides [7,8], and FN3 domains have been successfully expressed in prokaryotic, eukaryotic, intracellular, cell-surface and *in vitro* systems [1,11,15–29]. Crucially, ^{10}FN3 generally retains its thermal stability when its surface loops are replaced by those from other FN3 domains [30,31], indicating that it can tolerate extensive loop sequence variation. Batori *et al.* [32] explored the effects of modifying loop lengths on the overall stability of the ^{10}FN3 domain by inserting four to eight glycine residues into each loop and found that all except the EF loop could tolerate insertions without subsequent entropic penalties. Moreover, the combination of extended BC and FG loops resulted in only minor destabilization, suggesting that the domain can tolerate alterations over a large binding surface, as required for the construction of diverse libraries.

FN3 libraries

An ideal protein scaffold would accommodate a high degree of sequence variation while remaining highly stable, allowing target binding with high affinity and selectivity [2–4], and published data suggest that FN3 meets these criteria. FN3 libraries with randomized loops have successfully generated binders via phage display (M13 gene 3, gene 8; T7), mRNA display, yeast display and yeast two-hybrid systems, summarized in Fig. 2 and Table 1. Nearly all libraries have focused on the 'top' pole of the domain, which contains the BC, DE and FG loops. Libraries using only the FG loop have yielded molecules capable of discriminating between conformations of the estrogen receptor bound to different ligands [16,33] and between αvβ3 and α5β1 integrins, the latter using an FG loop with randomized residues flanking an integrin α5β1-binding Arg-Gly-Asp sequence from human ^{10}FN3 (RGD) sequence [17]. A crystal structure of the estrogen-receptor binding FN3 (PDB ID 2OCF; Fig. 3a) shows that the FG loop presents a short alpha

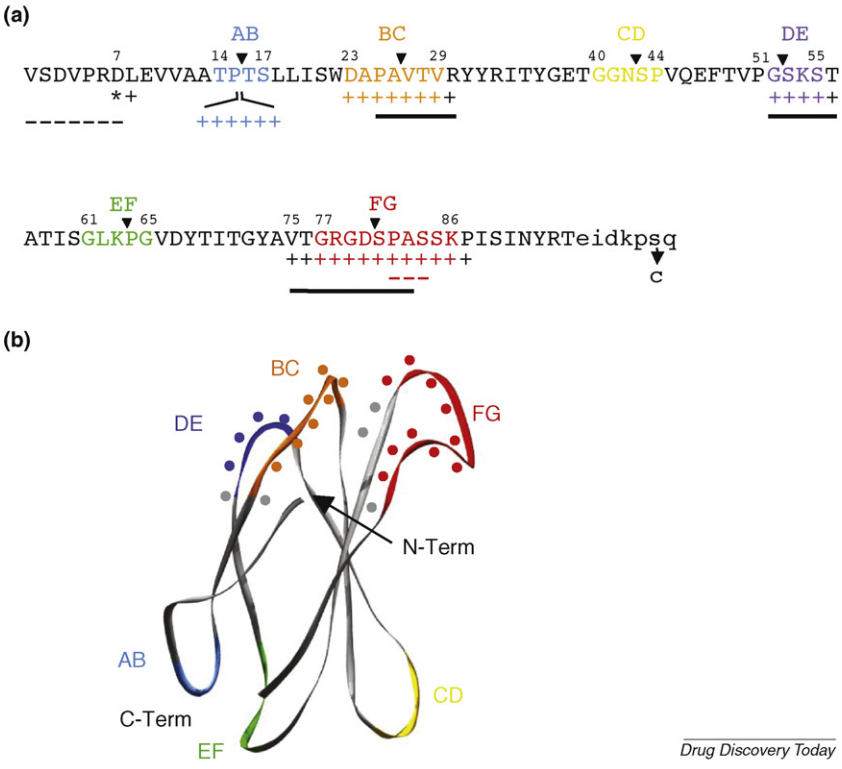

FIGURE 2

^{10}FN3 loop randomization. **(a)** Sequence of ^{10}FN3 showing positions that have been successfully altered in FN3 libraries. ^{10}FN3 loop residues are colored as in b. Positions that tolerate mutation or deletion are indicated by + and −, respectively. The bars under the BC and FG loops represent the amino acids replaced by loops of variable length in several libraries [11,22,23]. Positions mutated for biophysical property improvement are indicated by *, and the positions of glycine insertions described by Batori *et al.* [32] are indicated by ▼. The lower-case sequence denotes the natural linker between ^{10}FN3 and ^{11}FN3, and the position changed to cysteine for PEG addition and dimerization is indicated by the arrow [41]. **(b)** Ribbon representation of ^{10}FN3. The colored backbone segments represent FN loops. Positions randomized without structural disruption are marked with dots.

helix that extends outward toward its target, while the BC and DE loops, which were not randomized in the library, do not make close contact.

Libraries designed to cover a larger area have randomized the adjacent BC and FG loops, and some have also randomized the shorter DE loop (Table 1). These designs have enabled the isolation of binders with subnanomolar affinities. An mRNA display library with 21 residues randomized (7 in BC, 4 in DE and 10 in FG) was used to isolate FN3 binders to multiple targets with affinities as high as 0.09 nM after extensive selection without affinity optimization [20]. More recently, libraries allowing variation in the lengths of the loops (6–10, 4–10 and 8–14 amino acids in the BC, DE and FG loops, respectively [11,22,23]) have been introduced. Binding clones have been reported to use all available loop lengths, with the exception of the DE loop, for which only the four amino acid length of the parental ^{10}FN3 scaffold was selected [22]. When the DE loop and adjacent position 56 have been allowed to vary in sequence, however, different sequences are derived against different targets [11,20,22,34]. Crystal structures of four FN3 molecules (Fig. 3a) have shown relatively little direct participation of the DE loop in antigen binding [11,22,23], but when tested by mutation, the selected DE sequences are required for target binding [24,34].

These structures have indicated that FN3 loops can take on a variety of configurations, from convex surfaces [11] to extended single loops (see: 2OCF), without substantial alterations in the core structure (Fig. 3a). A crystal structure of a complex of the PDZ domain from erbin, its peptide ligand, and an FN3 selected from a library with variable loop lengths but limited amino acid diversity [23] showed that FN3 formed half of a 'clamshell' around the peptide (Fig. 3b), resulting in unusually high shape complementarities between the overall FN3 surface and the target. This study demonstrated the utility of adding an FN3 binding domain to augment an existing weak interaction, as well as the ability of a limited spectrum of amino acids to conform to an antigen surface. Interestingly, a yeast display selection of a BC–FG library has given rise to dominant clones with a single cysteine in each loop [18], potentially creating a disulfide bond that stabilizes an extended structure resembling the cleft-binding CDRs of camelid VHHs and shark IgNARs [12–14]. Thus, the growing body of experience with FN3 suggests that it behaves as a true protein scaffold, supporting modifications to its surface loops that allow the loop residues to accommodate binding interactions in multiple positions in space, while the central framework remains relatively unchanged (Fig. 3a). Furthermore, initial hopes that FN3 would accommodate a variety of molecular

TABLE 1

Characteristics of FN3 libraries

Reference	BC loop[a]	DE loop[a]	FG loop[a]	Other modifications	Display method	Library size	Randomization scheme[b]	Target	Highest affinity reported (nM)[c]
[16]			7 (78–84)		Two-hybrid	2×10^6	NNK/NNS	Estrogen receptor	High nM
[17]			5 (77–84)	$RGD_{78–80}$ fixed	Phage (pVIII)	1.5×10^9	NNK	Integrin αvβ3	0.8
[18]			7 (77–83)		Yeast	3×10^7	Trinucleotides; 20 aa equal	Hen egg lysozyme	610 (10)
[18]	7 (23–29)				Yeast	2×10^7	Trinucleotides; 20 aa equal	Hen egg lysozyme	(no binders)
[16]				AB loop + 7	Two-hybrid	2×10^5	NNK/NNS	Estrogen receptor	nd
[1]	5 (26–30)		5 (77–81, Δ 82–84)		Phage (pIII)	1×10^8	NNK	Ubiquitin	5000
[19]	5 (26–30)		5 (77–81, Δ 82–84)		Phage (pIII)	2×10^9	NNK	Src SH3	250
[20]	7 (23–29)		10 (77–86)		mRNA	1×10^{12}	NNS/preselect for ORFs	TNF-α, others	17
[18]	7 (23–29)		7 (77–83)		Yeast	5×10^7–6×10^8	Trinucleotides; 20 aa equal	Hen egg lysozyme	120 (0.35)
[21]	7 (23–29)		7 (77–83)		Phage T7	1×10^7	NNS	Streptavidin	nd
[20]	7 (23–29)	4 (52–55)	10 (77–86)		mRNA	1×10^{12}	NNS/preselect for ORFs	TNF-α, others	0.09 (0.02)
[22]	6–10 (25–30)	4–10 (52–55)	9–13 (75–83)	V29 fixed	Phage (pIII)/yeast	1×10^{10}	Y/S codons	MBP, hSUMO4, ySUMO	5
[11]	6–10 (25–30)	4–10 (52–55)	9–13 (75–83)	V29 fixed	Phage (pIII)/yeast		Mixture[d]	MBP	12
[23]	6–10 (25–30)	4 (52–55)[e]	8–14 (75–83)	N-terminal PDZ fusion	Phage (pIII)	1×10^9	Mixture[d]	ARVCF peptide	56 (4)
[27]	6–9 (23–30)	4–7 (52–56)	5–10 (77–86)		Yeast	6.5×10^7	NNB	Hen egg lysozyme	>1000 (.001)
[24]	None[f]	None[f]	10 (77–86)	Δ 1–7	mRNA		50% WT, 50% random nt	VEGFR2	(.06)
[25,28,35]	7 (23–29)		10 (77–86)	Δ 1–7	mRNA	3×10^{13}	NNS	Phospho-IκBα peptide; SARS N protein	18 (IκBα) 1.7 (SARS)

[a] BC, DE and FG loop randomization schemes: number of randomized residues (randomized amino acid positions based on Fig. 2a. In libraries with loop length variation, these numbers refer to positions replaced by variable-length randomized loops.)

[b] N = any nucleotide, S = G or C; K = G or T; B = G, T, or C.

[c] Affinities in parentheses refer to affinity-matured clones.

[d] BC and FG loops: trinucleotide codon mixture of 40% Y, 20% S, 10% G, 5% each A, D, H, L, N, R.

[e] DE loop = $((S/Y)_{52}(G/S/Y)_{53}(S/Y)_{54}(S/Y)_{55})$.

[f] BC, DE loop sequences fixed from parental VEGFR2 binding clone.

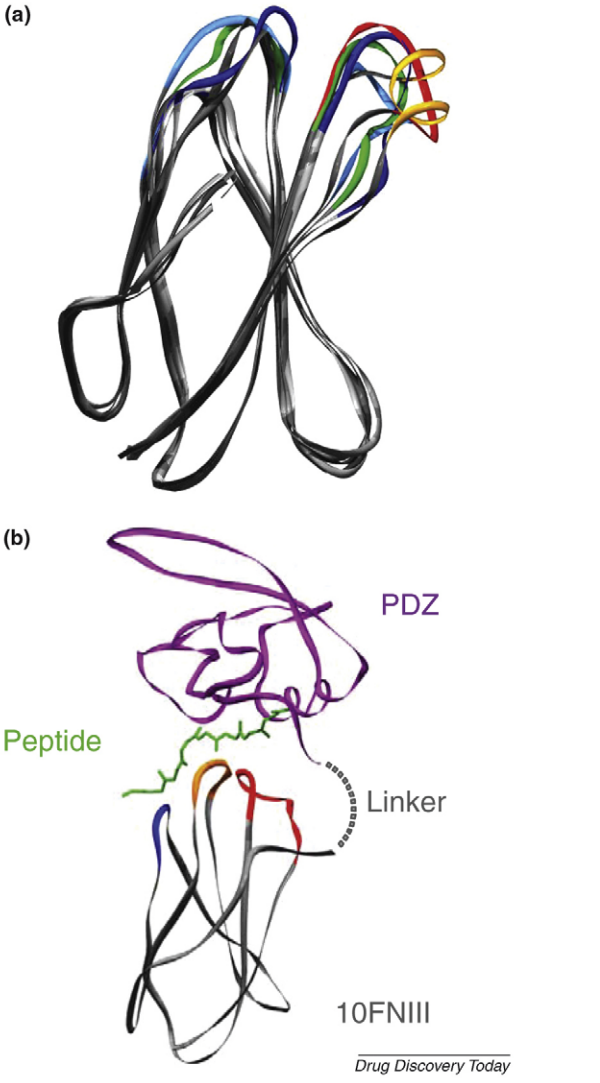

FIGURE 3

Engineered FN3 structures. **(a)** Overlay of wild-type ^{10}FN3 and ^{10}FN3 derived from loop randomization and selection. Yellow: FN3 selected for binding to human estrogen receptor alpha ligand-binding domain [16] (2OCF). Red: FN3 selected as fusion with erbin PDZ domain to bind ARCVF peptide [23] (2QBW). Green and blue: two FN3 domains selected for binding to MBP [11] (3CSB, 3CSG). Backbones of the randomized loops are shown in color for each molecule. **(b)** Crystal structure of FN3/PDZ fusion protein in complex with the ARVCF peptide, shown in green [23] (2QBW).

interactions analogous to those of antibodies appear to be well founded.

Relatively little attention has been paid to the 'bottom' pole of ^{10}FN3. One library containing seven randomized amino acids inserted into the AB loop was used to identify a binder to estrogen receptor in a yeast-two hybrid system [16], but the function of this FN3 outside the yeast two-hybrid context has not been reported. No CD loop library has been described, but both the stability studies of Batori *et al.* [32] and the diversity of conformations and binding interactions seen in natural CD loops ([9,10] Fig. 1b) suggest that this loop could be the basis for the development of additional binding activities, thereby allowing for bispecific single-domain molecules.

Extending the range of FN3 binding beyond three loops

In the 3D structure of ^{10}FN3, the N-terminus is in close proximity to the BC and FG loops (Fig. 2b) and could interfere with target binding, a theory supported by the observation that a deletion of the first seven amino acids improved binding of FN3s to vascular endothelial growth factor receptor 2 (VEGFR2) by about threefold [24]. Olson and Roberts [25] also found that the stability of a mutant ^{10}FN3 lacking amino acids one to seven is identical to that of wild-type ^{10}FN3, and several libraries lacking codons one to seven have been used successfully [24,25,28,35].

Others have taken advantage of the N-terminus to generate new sites of interaction. FN3 domains naturally exist with additional protein domains at the N and C termini and in some cases use amino acids from adjacent domains or in the inter-domain linker between tandem FN3 domains to participate in ligand binding [10]. In display systems, functional FN3 has been fused to other protein domains or nucleic acids at either its N-terminus [11,16,18,21,22,23,27,28,36] or its C-terminus [1,15,17,19,20,22,23,26,37]. Tani *et al.* [38] reported the phage display selection of a ^{9}FN3–^{10}FN3 unit, using random mutagenesis to identify sequences that modified integrin binding. Selection of tandem FN3 libraries with randomized loops has not been reported, but the library described by Huang *et al.* [23] contained a 96-amino acid PDZ domain fused to the N-terminus of a randomized FN3 and was selected for enhanced binding to the peptide target of the PDZ domain. In this case, the selected FN3 domain by itself did not show detectable binding to the peptide, but when compared with the parental PDZ domain, the fusion protein had 500-fold increased affinity to the peptide (4 nM versus 2.2 μM) and 2000-fold greater selectivity for the target peptide over a related peptide. A phospho-peptide-binding FN3 selected by mRNA display [28] retained its function in several engineered forms following selection. The most complex of these is a fusion of cyan fluorescent protein (CFP), FN3, the substrate peptide sequence and yellow fluorescent protein (YFP), which gives a fluorescence resonance energy transfer (FRET) signal when the substrate is phosphorylated. The high tolerance of both natural and engineered FN3 for the presence of additional sequences at each end points to the great promise of this scaffold to form the basis of more complex molecules, which is particularly useful for therapeutic proteins requiring several functionalities to be brought into one molecule.

Affinity optimization

In general, the maximum affinity of clones derived from a library is believed to be a function of the amount of sequence space randomized and the number of diverse clones in the library [39], which in turn is limited by the display system used. Gilbreth *et al.* [11] compared FN3s selected for binding to maltose-binding protein (MBP) from libraries built with a minimal sequence diversity (tyrosine/serine) and an expanded sequence diversity (tyrosine/serine and a set of amino acids (glycine, alanine, aspartic acid, histidine, leucine, asparagine and arginine) with a mixture of different properties–charge, hydrophobicity, polarity, size and conformational flexibility–to accommodate various binding sites) and obtained the crystal structures of two binders with nearly identical epitopes. Not only did the more sequence-diverse library

generate a higher affinity clone (12 nM versus 73 nM), but it expanded both the number of BC loop residues involved in the binding interaction and the tolerance of individual loop positions for further mutation.

FN3 domains with subnanomolar affinity, comparable to the levels achieved with conventional single-chain variable fragment of IgG (scFv) or antigen-binding fragment of IgG (Fab)s, have frequently been obtained following affinity optimization (Table 1). Xu *et al.* [20] applied error-prone PCR to a pool of tumor necrosis factor-α (TNF-α)-binding FN3s and increased the maximum affinity in the population from 1 nM to 20 pM. Mutations were found in both loops and frameworks, but the effects of framework mutations on affinity and stability were not reported. More recently, Getmanova *et al.* [24] described affinity improvement of a VEGFR2-binding FN from 11 nM to 0.32 nM and simultaneous introduction of cross-reactivity to murine VEGFR2 using a library in which the FG loop sequence had equal proportions of parental and random nucleotides incorporated at each position. The alternative strategy of holding the FG loop constant and completely randomizing the BC loop has also proven successful, generating affinity increases of 10–300 fold [18,23].

FN3 domains have also been combined after engineering as monomers to generate molecules with higher avidity or multiple specificities. Duan *et al.* [40] showed that a pentamerization domain, the COMP peptide, could be fused at the C-terminus of an integrin αvβ3-binding FN3 to enhance apparent affinity by 500-fold. A recently published patent application from Adnexus [41] describes the use of C-terminal cysteines (Fig. 2a) to couple two FN3 domains directly by a disulfide or indirectly via a branched polyethylene glycol (PEG) molecule, the latter approach also being used to link two FN3 domains directed against different targets, with retention of activity against both targets.

FN3 domain stability

The molecules emerging from library screening and subsequent optimization generally retain a high level of stability by several measurements. Richards *et al.* [17] reported that their integrin-binding FN3, derived from FG loop randomization, maintained 80% of its activity following a 24-hour incubation at 75°C, and Huang *et al.* [23] showed that a PDZ–FN3 fusion protein from a three-loop library remained monomeric and active after two hours at 50°C. FN3 variants retain binding function in multiple conditions, including after immobilization and drying onto a glass slide [20] or coupling to an In_2O_3 nanowire [29] for use as target-detection reagents. More detailed analyses have shown that clones selected on the basis of binding alone can have significant destabilization compared to wild-type ^{10}FN3, but that single amino acid changes can dramatically reinstate stability and solubility, generating molecules with melting temperatures above 60°C and soluble *E. coli* expression above 20 mg/L [24,34,42]. Dutta *et al.* [36] have used the ability of independently expressed fragments of FN3 (amino acids 1–42 and 43–94, split in the CD loop) to assemble on the surface of yeast cells as the basis of a screen for variants with improved stability. Overall, stability data reported so far indicate that modified FN3 can have thermal stability as high as, or higher than that of, immunoglobulins suggesting that FN3 bearing a variety of large modifications to the loop regions may refold easily and survive the harsh conditions demanded by some therapeutic or diagnostic applications.

FN3 as a pharmaceutical scaffold

The library work to date has shown that the tools are in place for rapid generation of high-affinity stable FN molecules capable of potent function *in vitro*. A few, including a recently described set of FN3 molecules capable of inhibiting SARS virus replication when expressed intracellularly [35], block biological functions in cell culture. The test case for the *in vivo* behavior of FN3 is CT-322, a VEGFR2-binding FN3 (derived from molecules described in Refs. [24,34]), currently in clinical development by Bristol-Myers Squibb. The major concerns about using a novel small protein scaffold as a therapeutic are – clinical efficacy aside – its expected rapid clearance from circulation and the potential for creating an immune response. The CT-322 FN3 domain is coupled via a C-terminal cysteine (Fig. 2a) to a 40-kDa PEG to increase the size of the molecule above the threshold for kidney-mediated clearance [43]. In preclinical studies, CT-322 blocks the angiogenic activity of VEGF *in vitro* and has shown efficacy in human tumor xenograft models [44]. In a Phase I study in patients with solid tumors, CT-322 administered intravenously at 1 mg/kg showed a terminal half-life of 68.7 hours, based on the first dose of a weekly dosing regimen [45,46]. The half-life in humans is substantially shorter than that of IgG (7–26 days [47]), as expected for a molecule lacking FcRn binding, and also shorter than the 14-day half-life reported for Cimzia, a pegylated Fab that binds to TNF-α [48]. Still, the pharmacokinetics of CT-322 supported weekly intravenous dosing, and a biomarker for VEGFR2 blockade showed sustained elevation over several repeated weekly doses. Phase I trial data also showed that CT-322 is tolerated up to a maximum dose of 2 mg/kg without clinically significant immunogenicity [45,46]. Patients are currently being enrolled in a Phase II trial in glioblastoma multiforme, in which CT-322 will be tested alone or in combination with irinotecan.

Conclusion

A decade after publication of the first proof of concept, FN3 is proving to be a robust scaffold for use in multiple display formats. Affinities as high as those achieved by conventional antibodies are possible, and early experiments suggest that the range of molecular interactions that can be targeted by FN3 is likely to be broad, owing to the capacity of the scaffold to accept diverse loop lengths and also coupling to other protein domains. PEGylation has shown to be suitable for the enhancement of pharmacokinetics of this 10-kDa domain. The first human trials of a PEGylated FN3 are underway, and initial safety and pharmacokinetic profiles have allowed progression to a Phase II study. The data that emerge from this trial will be an important test of the proposition that a small, stable scaffold that can be engineered to possess good drug-like properties *in vitro* will retain sufficiently good pharmacokinetics and stability to perform in the clinic.

Conflicts of interest

Laird Bloom is a former employee of Phylos, Inc., a predecessor of Adnexus, now a part of Bristol-Myers Squibb.

Acknowledgements

The authors would like to thank Shohei Koide and Ryan Gilbreth for sharing structures and manuscripts before publication, Samta Kundu for providing conference presentations on CT-322 and Jonny Finlay for a critical reading of this manuscript.

References

1 Koide, A. *et al.* (1998) The fibronectin type III domain as a scaffold for novel binding proteins. *J. Mol. Biol.* 284, 1141–1151
2 Skerra, A. (2007) Alternative non-antibody scaffolds for molecular recognition. *Curr. Opin. Biotechnol.* 18, 295–304
3 Gebauer, M. and Skerra, A. (2009) Engineered protein scaffolds as next-generation antibody therapeutics. *Curr. Opin. Chem. Biol.* 13, 1–11
4 Gill, D.S. and Damle, N.K. (2006) Biopharmaceutical drug discovery using novel protein scaffolds. *Curr. Opin. Biotechnol.* 17, 653–658
5 Fraser, J.S. *et al.* (2006) Ig-like domains on bacteriophages: a tale of promiscuity and deceit. *J. Mol. Biol.* 59, 496–507
6 Dickinson, C.D. *et al.* (1994) Crystal structure of the tenth type III cell adhesion module of human fibronectin. *J. Mol. Biol.* 236, 1079–1092
7 Litvinovich, S.V. and Ingham, K.C. (1995) Interactions between type III domains in the 110 kDa cell-binding fragment of fibronectin. *J. Mol. Biol.* 248, 611–626
8 Cota, E. *et al.* (2001) The folding nucleus of a fibronectin type III domain is composed of core residues of the immunoglobulin-like fold. *J. Mol. Biol.* 305, 1185–1194
9 Wang, X. *et al.* (2005) Structure of the quaternary complex of interleukin-2 with its alpha, beta, and gammac receptors. *Science* 310, 1159–1163
10 Somers, W. *et al.* (1994) The x-ray structure of a growth hormone-prolactin receptor complex. *Nature* 372, 478–481
11 Gilbreth, R.N. *et al.* (2008) A dominant conformational role for amino acid diversity in minimalist protein–protein interfaces. *J. Mol. Biol.* 381, 407–418
12 Koide, A. *et al.* (2007) Exploring the capacity of minimalist protein interfaces: interface energetics and affinity maturation to picomolar K_D of a single-domain antibody. *J. Mol. Biol.* 373, 941–953
13 Stanfield, R.L. *et al.* (2007) Maturation of shark single-domain (IgNAR) antibodies: evidence for induced-fit binding. *J. Mol. Biol.* 367, 358–372
14 Henderson, K.L. *et al.* (2007) Structure of an IgNAR–AMA1 complex: targeting a conserved hydrophobic cleft broadens malarial strain recognition. *Structure* 15, 1452–1466
15 Koide, A. and Koide, S. (2007) Monobodies: antibody mimics based on the scaffold of the fibronectin type III domain. *Methods Mol. Biol.* 352, 95–109
16 Koide, A. *et al.* (2002) Probing protein conformational changes in living cells by using designer binding proteins: application to the estrogen receptor. *Proc. Natl. Acad. Sci. U. S. A.* 99, 1253–1258
17 Richards, J. *et al.* (2003) Engineered fibronectin type III domain with a RGDWXE sequence binds with enhanced affinity and specificity to human alphavbeta3 integrin. *J. Mol. Biol.* 326, 1475–1488
18 Lipovsek, D. *et al.* (2007) Evolution of an interloop disulfide bond in high-affinity antibody mimics based on fibronectin type III domain and selected by yeast surface display: molecular convergence with single-domain camelid and shark antibodies. *J. Mol. Biol.* 368, 1024–1041
19 Karatan, E. *et al.* (2004) Molecular recognition properties of FN3 monobodies that bind the Src SH3 domain. *Chem. Biol.* 11, 835–844
20 Xu, L. *et al.* (2002) Directed evolution of high-affinity antibody mimics using mRNA display. *Chem. Biol.* 9, 933–942
21 Garcia-Ibilcieta, D. *et al.* (2008) Simple method for production of randomized human tenth fibronectin domain III libraries for use in combinatorial screening procedures. *Biotechniques* 44, 559–562
22 Koide, A. *et al.* (2007) High-affinity single-domain binding proteins with a binary-code interface. *Proc. Natl. Acad. Sci. U. S. A.* 104, 6632–6637
23 Huang, J. *et al.* (2008) Design of protein function leaps by directed domain interface evolution. *Proc. Natl. Acad. Sci. U. S. A.* 105, 6578–6583
24 Getmanova, E.V. *et al.* (2006) Antagonists to human and mouse vascular endothelial growth factor receptor 2 generated by directed protein evolution in vitro. *Chem. Biol.* 13, 549–556
25 Olson, C.A. and Roberts, R.W. (2007) Design, expression, and stability of a diverse protein library based on the human fibronectin type III domain. *Protein Sci.* 16, 476–484
26 Bertschinger, J. and Neri, D. (2004) Covalent DNA display as a novel tool for directed evolution of proteins in vitro. *Protein Eng. Des. Sel.* 17, 699–707
27 Hackel, B.J. *et al.* (2008) Picomolar affinity fibronectin domains engineered utilizing loop length diversity, recursive mutagenesis, and loop shuffling. *J. Mol. Biol.* 381, 1238–1252
28 Olson, C.A. *et al.* (2008) mRNA display selection of a high-affinity, modification-specific phospho-IκBα-binding fibronectin. *ACS Chem. Biol.* 3, 480–485
29 Ishikawa, F.N. *et al.* (2009) Label-free, electrical detection of the SARS virus N-protein with nanowire biosensors utilizing antibody mimics as capture probes. *ACSNano* 3, 1219–1224
30 Siggers, K. *et al.* (2007) Conformational dynamics in loop swap mutants of homologous fibronectin type III domains. *Biophys. J.* 93, 2447–2456
31 Billings, K.S. *et al.* (2008) Crosstalk between the protein surface and hydrophobic core in a core-swapped fibronectin type III domain. *J. Mol. Biol.* 375, 560–571
32 Batori, V. *et al.* (2002) Exploring the potential of the monobody scaffold: effects of loop elongation on the stability of a fibronectin type III domain. *Protein Eng.* 12, 1015–1020
33 Huang, J. *et al.* (2006) Conformation-specific affinity purification of proteins using engineered binding proteins: application to the estrogen receptor. *Protein Expr. Purif.* 47, 348–354
34 Parker, M.H. *et al.* (2005) Antibody mimics based on human fibronectin type three domain engineered for thermostability and high-affinity binding to vascular endothelial growth factor receptor two. *Protein Eng. Des. Sel.* 18, 435–444
35 Liao, H.I. *et al.* (2009) mRNA display of fibronectin-based intrabodies that detect and inhibit SARS-COV N protein. *J. Biol. Chem.* http://www.jbc.org/cgi/doi/10.1074/jbc.M901547200
36 Dutta, S. *et al.* (2005) High-affinity fragment complementation of a fibronectin type III domain and its application to stability enhancement. *Protein Sci.* 14, 2838–2848
37 Han, Z. *et al.* (2004) Accelerated screening of phage-display output with alkaline phosphatase fusions. *Comb. Chem. High Throughput Screen.* 7, 55–62
38 Tani, P.H. *et al.* (2004) In vitro selection of fibronectin gain-of-function mutations. *Biochem. J. X* 365, 287–294
39 Lipovsek, D. and Plückthun, A. (2004) In-vitro protein evolution by ribosome display and mRNA display. *J. Immunol. Methods* 290, 51–67
40 Duan, J. *et al.* (2007) Fibronectin type III domain based monobody with high avidity. *Biochemistry* 46, 12656–12664
41 Camphausen, Ray *et al.* Adnexus. Targeted therapeutics based on engineered proteins for tyrosine kinases receptors, including igf-ir. *WO2008066752* (A2)
42 Koide, A. *et al.* (2001) Stabilization of a fibronectin type III domain by the removal of unfavorable electrostatic interactions on the protein surface. *Biochemistry* 40, 10326–10333
43 Mamluk, R. *et al.* (2006) Abstract. *Proc. Am. Assoc. Cancer Res.* 47, 230
44 Dineen, S.P. *et al.* (2008) The Adnectin CT-322 is a novel VEGF receptor 2 inhibitor that decreases tumor burden in an orthotopic mouse model of pancreatic cancer. *BMC Cancer* 10.1186/1471-2407-8-352 http://www.biomedcentral.com
45 Sweeney, C.J. *et al.* (2008) Abstract. *J. Clin. Oncol.* 26 (20 Suppl.), 2523
46 Molckovsky, A. and Siu, L.L. (2008) First-in-class, first-in-human phase I results of targeted agents: Highlights of the 2008 American Society of Clinical Oncology Meeting. *J. Hematol. Oncol.* 10.1186/1756-8722-1-20 http://www.jhoonline.org
47 Tang, L. *et al.* (2004) Pharmacokinetic aspects of biotechnology products. *J. Pharm. Sci.* 93, 2184–2204
48 Choy, E.H. *et al.* (2002) Efficacy of a novel PEGylated humanized anti-TNF fragment (CDP870) in patients with rheumatoid arthritis: a phase II double-blinded, randomized, dose-escalating trial. *Rheumatology (Oxford)* 41, 1133–1137